The EMBO Journal Vol.18 No.11 pp.2911–2922, 1999

Crystal structure of two CD46 domains reveals an extended measles virus-binding surface

José M.Casasnovas, Mykol Larvie[1] and Thilo Stehle[2,3]

Department of Biosciences at NOVUM, Karolinska Institute, 14157 Huddinge, Sweden, [1]Graduate Program in Biological and Biomedical Sciences, Harvard Medical School, and Harvard–MIT Division of Health Sciences and Technology, Cambridge, MA 02139 and [2]Laboratory of Developmental Immunology, Massachusetts General Hospital and Harvard Medical School, 55 Fruit Street, Boston, MA 02114, USA

[3]Corresponding author
e-mail: stehle@fluxus.mgh.harvard.edu

Measles virus is a paramyxovirus which, like other members of the family such as respiratory syncytial virus, is a major cause of morbidity and mortality worldwide. The cell surface receptor for measles virus in humans is CD46, a complement cofactor. We report here the crystal structure at 3.1 Å resolution of the measles virus-binding fragment of CD46. The structure reveals the architecture and spatial arrangement of two glycosylated short consensus repeats with a pronounced interdomain bend and some flexibility at the domain interface. Amino acids involved in measles virus binding define a large, glycan-free surface that extends from the top of the first to the bottom of the second repeat. The extended virus-binding surface of CD46 differs strikingly from those reported for the human virus receptor proteins CD4 and intercellular cell adhesion molecule-1 (ICAM-1), suggesting that the CD46 structure utilizes a novel mode of virus recognition. A highly hydrophobic and protruding loop at the base of the first repeat bears a critical virus-binding residue, thereby defining an important recognition epitope. Molecules that mimic the conformation of this loop potentially could be effective anti-viral agents by preventing binding of measles virus to CD46.

Keywords: CD46/measles virus/membrane cofactor protein/short consensus repeat/virus–receptor interaction

Introduction

Human CD46, also known as membrane cofactor protein (MCP), is a widely expressed glycoprotein that is present on most cells, including lymphocytes, granulocytes, monocytes, platelets, endothelial cells, epithelial cells and fibroblasts (Seya *et al*., 1986; Lublin *et al*., 1988). The molecule protects host cells from autoimmune destruction by binding to complement proteins C3b and C4b at the cell surface and serving as a cofactor for their cleavage by factor I, a serine protease (Seya *et al*., 1986; Liszewski *et al*., 1991). CD46 belongs to a family known as the regulators of complement activation (RCA), which also includes decay-accelerating factor (DAF/CD55), the complement receptors 1 (CR1/CD35) and 2 (CR2/CD21), the C4-binding protein and factor H (Liszewski *et al*., 1991). The proteins in this family contain 'short consensus repeats' (SCRs), modules of ~60 amino acids with four invariant cysteines and a small number of additional conserved residues (Liszewski *et al*., 1991). SCR domains are present in many complement regulatory proteins as well as in a large number of other cell surface proteins, including interleukin (IL)-2 receptor, β2-glycoprotein, proteoglycan core protein, haptoglobin 2 and the selectins (Bork *et al*., 1996). NMR analyses of fragments of factor H (FcH, Barlow *et al*., 1993) and the vaccinia virus complement control protein (VCP; Wiles *et al*., 1997) have established that SCR domains adopt a β-barrel structure. The CD46 ectodomain contains four SCRs and a region rich in serine, threonine and proline (STP region), followed by a transmembrane segment and a short cytoplasmic tail at the C-terminus. Domains SCR1, SCR2 and SCR4 each have one *N*-linked carbohydrate moiety, and the STP region contains *O*-linked glycosylation. Although the molecule is normally membrane bound, soluble forms of CD46 are present in tears, plasma and reproductive tract fluids (Hara *et al*., 1992; McLaughlin *et al*., 1996). Recent studies have shown that recombinant soluble CD46 inhibits complement activation, suggesting a potential role for the molecule as a therapeutic agent (Christiansen *et al*., 1996).

Apart from their role in complement regulation, several members of the RCA family also function as virus receptors: CD21 is a receptor for Epstein–Barr virus (Fingeroth *et al*., 1984), CD55 serves as a receptor for several echoviruses and some coxsackieviruses (Bergelson *et al*., 1994, 1997; Ward *et al*., 1994) and CD46 is the receptor for at least two measles virus strains (Dörig *et al*., 1993; Naniche *et al*., 1993). In all three cases, formation of the virus–receptor complex requires the presence of two or more consecutive SCRs (Molina *et al*., 1991; Clarkson *et al*., 1995; Iwata *et al*., 1995; Manchester *et al*., 1995). For CD46, the two N-terminal repeats are sufficient for binding of the receptor to measles virus (Iwata *et al*., 1995; Manchester *et al*., 1995). Competitive inhibition studies identified two short CD46 peptides that presumably interact with measles virus (Manchester *et al*., 1997). This information, combined with site-directed mutagenesis experiments (Buchholz *et al*., 1997; Hsu *et al*., 1997), revealed the presence of two virus-binding sites, one in SCR1 and one in SCR2. In contrast, the complement-binding regions of CD46 have been mapped to SCR2, SCR3 and SCR4 (Adams *et al*., 1991).

The measles virus hemagglutinin is an integral membrane glycoprotein that binds to CD46 and mediates attachment of the virus to host cells (Nussbaum *et al*., 1995; Griffin and Bellini, 1996). The interaction between CD46 and measles virus is thought to inhibit the production

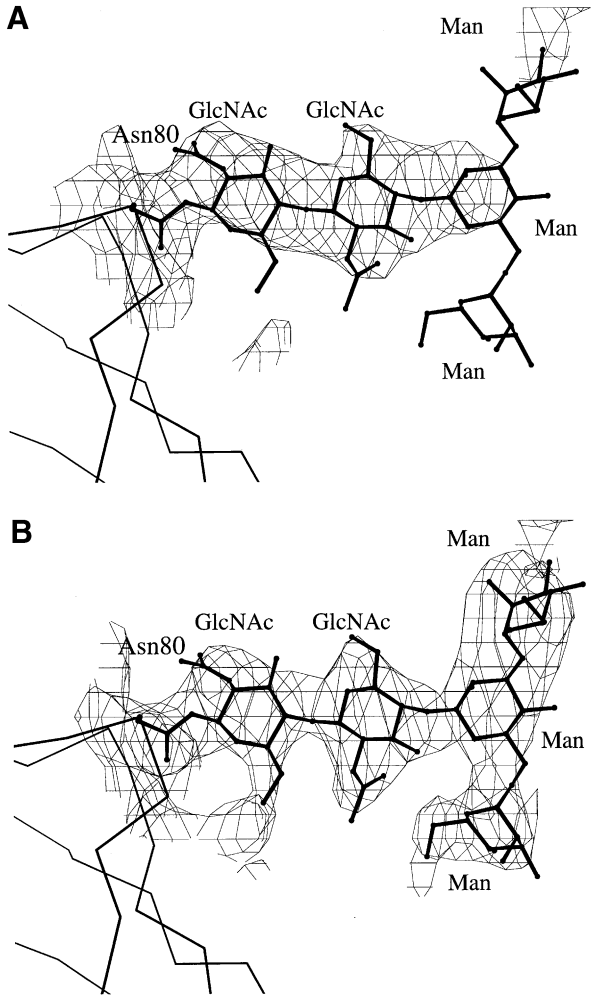

Fig. 1. Electron density maps showing the *N*-linked glycan attached to Asn80 in SCR2. The refined model is shown. (**A**) Averaged electron density map at 3.4 Å resolution (see Materials and methods). (**B**) $2F_o–F_c$ map at 3.1 Å resolution, calculated with phases obtained from the final model. Because they participate in crystal contacts, an unusually large number of sugar residues are relatively well ordered and have therefore been included in the model. Contours are at 2.0 σ (A) and 1.0 σ (B).

of IL-12 by monocytes, contributing in part to the profound suppression of cell-mediated immunity that occurs in patients infected with measles virus (Karp *et al*., 1996). Although several hemagglutinin residues recently have been implicated in binding to CD46 (Hsu *et al*., 1998; Patterson *et al*., 1999), little is known about this interaction and no structural information about the hemagglutinin is available.

In order to understand better how CD46 interacts with measles virus, and to study the role of short consensus repeats as virus receptors, we used X-ray crystallography to determine the structure of the measles virus-binding region of CD46. This crystal structure is the first of a molecule that contains SCRs, and it provides information that is essential for the further characterization of SCR domains and their function in complement regulation and virus recognition. The availability of the three-dimensional structure allows a detailed interpretation of previously reported mutagenesis and virus-binding studies. Our analysis of the structure indicates that measles virus binds to an extended surface formed by two flexibly linked CD46 domains. We identify a highly hydrophobic loop that protrudes markedly from the center of this surface and is likely to play an important role in the interaction with the virus. A comparison of the virus-binding surface of CD46 with those reported for human CD4 and human intercellular cell adhesion molecule-1 (ICAM-1) reveals a substantial difference in their virus recognition modes. We conclude that the interaction between CD46 and measles virus is the first example of a novel type of virus–receptor interaction that is likely to be shared by other virus receptors within the RCA family.

Results and discussion

Structure determination and model accuracy

A soluble fragment comprising the two N-terminal SCRs of human CD46 was expressed in lectin-resistant Chinese hamster ovary (CHO) Lec 3.2.8.1 cells (Stanley, 1989) in order to obtain a homogeneous, high-mannose glycoform (see Materials and methods). The crystallized protein consists of 126 residues and two *N*-linked high-mannose carbohydrates. The structure of the fragment was determined by X-ray crystallography with the use of multiple isomorphous replacement (Table I; Materials and methods). Because the crystals contain six nearly identical copies of the molecule in their asymmetric unit, we were able to improve significantly the initial phases through non-crystallographic symmetry electron density averaging (Kleywegt and Jones, 1994). The six molecules have very similar crystal contacts, and they assemble into a dimer of trimers that is discussed in more detail below. The model was built using O (Jones *et al*., 1991) into domain-wise averaged maps and refined at 3.1 Å with X-PLOR (Brünger *et al*., 1987). Examples of the 6-fold averaged and the final $2F_o–F_c$ electron density maps are shown in Figure 1. The crystallographic *R*-factor for the present model and all available data between 20 and 3.1 Å is 24.4%; the corresponding free *R*-factor (Brünger, 1992) for 3% of the data (765 reflections) is 29.8%. The model has good geometry, with small root-mean-square deviations from ideal values for bond lengths (0.015 Å) and bond angles (2.4°). PROCHECK (CCP4, 1994) analysis shows no outliers in the Ramachandran plot.

Overall structure

The structure of the N-terminal two short consensus repeats of CD46 is shown in Figure 2A. The polypeptide chain folds into two concatenated β-barrels, each containing two disulfide bonds and one *N*-linked glycan attached to the 'top' of the domain. The two glycans cover a significant portion of the concave side of the molecule and approach each other due to a pronounced bend of ~60° between the two domains (Figure 2A).

The β-barrel in each repeat consists of a four-stranded antiparallel β-sheet formed by strands B, C, D and E, a proline-containing segment between strands E and E′ at the edge of the sheet, and a two-stranded β-sheet with strands D′ and E′ at the base of the barrel (Figure 2A and B). On one side of the barrel, the four-stranded central β-sheet packs against an extended N-terminal coil structure. An additional short β-sheet composed of strands A and B′ is present at the top of SCR2. This sheet is

Table I. Data collection and phasing statistics

	Native	$KAuCl_4$	K_2PtCl_6	K_2OsO_4	$KAuCl_4$	K_2PtCl_6
Data collection						
Soak[a] (mM)	–	1	1	1	0.5	0.4
Resolution[b] (Å)	20–3.1 (3.3–3.1)	20–3.4 (3.5–3.4)	20–3.5 (3.6–3.5)	20–4.0 (4.2–4.0)	20–3.9 (4.0–3.9)	20–4.0 (4.1–4.0)
Coverage[c] (%)	92.6 (68.1)	92.7 (88.4)	88.1 (89.9)	92.5 (90.2)	97.2 (97.1)	97.8 (86.3)
R_{merge}[d] (%)	4.9 (29.0)	10.8 (33.8)	8.9 (35.6)	9.9 (27.3)	11.5 (34.2)	9.6 (27.9)
$I/\sigma(I)$	18.5 (3.1)	9.5 (1.9)	12.2 (2.9)	13.2 (5.0)	9.9 (2.9)	11.9 (3.9)
Phasing						
R_{nat}[e] (%)	–	45.7	43.7	24.1	38.3	29.3
No. of sites	–	6	12	16	17	12
Phasing power	–	1.35	1.72	1.12	1.51	1.92

[a]Concentration of heavy atom compound in soak buffer.
[b]Data in parentheses pertain to the highest resolution bin.
[c]Coverage (number of independent reflections/theoretical number possible).
[d]$R_{merge} = \Sigma|I - <I>|/\Sigma I$, where I is the observed intensity and $<I>$ is the average intensity from multiple observations of symmetry-related reflections.
[e]$R_{nat} = \Sigma|F_{PH} - F_P|/\Sigma (F_{PH} + F_P)$, where F_P = protein structure factor amplitude and F_{PH} = heavy atom derivative structure factor amplitude.

absent in SCR1, although the first residue in SCR1 is hydrogen bonded to a residue in the loop between strands B and C (BC-loop) in a β-sheet-like fashion (Figure 2B). SCR1 also contains a short piece of 3_{10}-helix that leads into strand E′. The two β-barrels face towards opposite directions (Figure 2A and B), requiring a rotation of close to 180° along the long axis of one domain to superimpose it with the other.

Arrangement of the molecules in the crystal

The six independent CD46 SCR1–SCR2 molecules assemble into a surprising oligomeric structure in the crystals. Three SCR1 domains form a ring-like unit that features extensive intermolecular interactions (Figure 2C). With the three corresponding SCR2 domains protruding from one side of the ring, this arrangement resembles a three-legged table. The 'tabletop', which is formed mainly by strands B and C of SCR1, is almost perfectly planar and entirely devoid of glycosylation. The tabletops of two very similar tables stack upside down against each other, giving rise to a hexameric arrangement of the molecules in the asymmetric unit (Figure 2C, inset). An essentially identical hexameric structure is present in a completely unrelated crystal form of CD46 SCR1–SCR2 (M.Larvie, J.M.Casasnovas and T.Stehle, unpublished results).

The hydrophobic character and the amount of surface area buried in each trimer contact of CD46 (see legend to Figure 2C) is similar, for example, to the intermolecular contact reported for human ICAM-1, which exists as a dimer at the cell surface (Casasnovas *et al*., 1998). Although presently there is no evidence for biologically relevant oligomerization of CD46, the trimeric arrangement that we observe independently in two crystal forms suggests that CD46 might form such a trimer at the cell surface.

Interdomain interface

The two repeats of CD46 are highly compact domains. With a buried surface area of 360 Å^2, the interdomain interface shields only a small fraction (~4%) of the molecular surface of each repeat from solvent. Four residues (Tyr61–Arg62–Glu63–Thr64) at the interface join the C-terminal cysteine of SCR1 to the first cysteine of SCR2 (Figure 3A). Tyr61 is firmly anchored to SCR1 by two hydrogen bonds to Phe35 in strand D′ (Figure 2B). Similarly, Glu63 forms a hydrogen bond with Phe85 in strand B′ of SCR2 and is, therefore, an integral part of the second repeat. There are relatively few interdomain contacts, and Arg62, the terminal residue in strand E′ of SCR1, accounts for a large proportion of them (Figure 3A).

The interdomain interface contains a calcium ion that is coordinated to two aspartic acids (Asp57 and Asp58) at the base of SCR1 (Figure 3A). Although it does not interact directly with residues in SCR2, solvent-mediated contacts between this ion and residues in SCR2 could stabilize the interdomain interface and restrict interdomain movement (see below). The requirement for calcium for crystallization (see Materials and methods) strongly supports this hypothesis. However, it is not known at this time whether divalent cations play a role in the interaction of CD46 with its ligands.

Interdomain movement

The comparison of the six independent copies of the molecule in the asymmetric unit reveals some flexibility at the interdomain interface (Figure 3B), which is consistent with the small surface area buried at the interface, and with the few observed interdomain contacts. The interdomain angle varies by ~15° among the six copies, and the movement is mostly in a direction perpendicular to the first disulfide bridge in SCR2. There is no single hinge residue to which the interdomain movement can be assigned; rather, the differences are absorbed by small changes in conformation of three amino acids (Tyr61, Arg62 and Glu63). The movement at the interface is probably somewhat restricted by the crystal contact between the interdomain interface of one molecule and the tip of SCR1 from a neighboring molecule discussed above (Figure 2C).

Structural comparison of SCR domains and interdomain orientations

The structural alignment of the two SCR modules of CD46 presented in Figure 4A shows good superposition for many residues in the central β-sheet but significant differences for most of the remaining regions of the molecule. Residues in the central β-sheet of SCR1 align well with residues in the same region of SCR2 in CD46, and also with

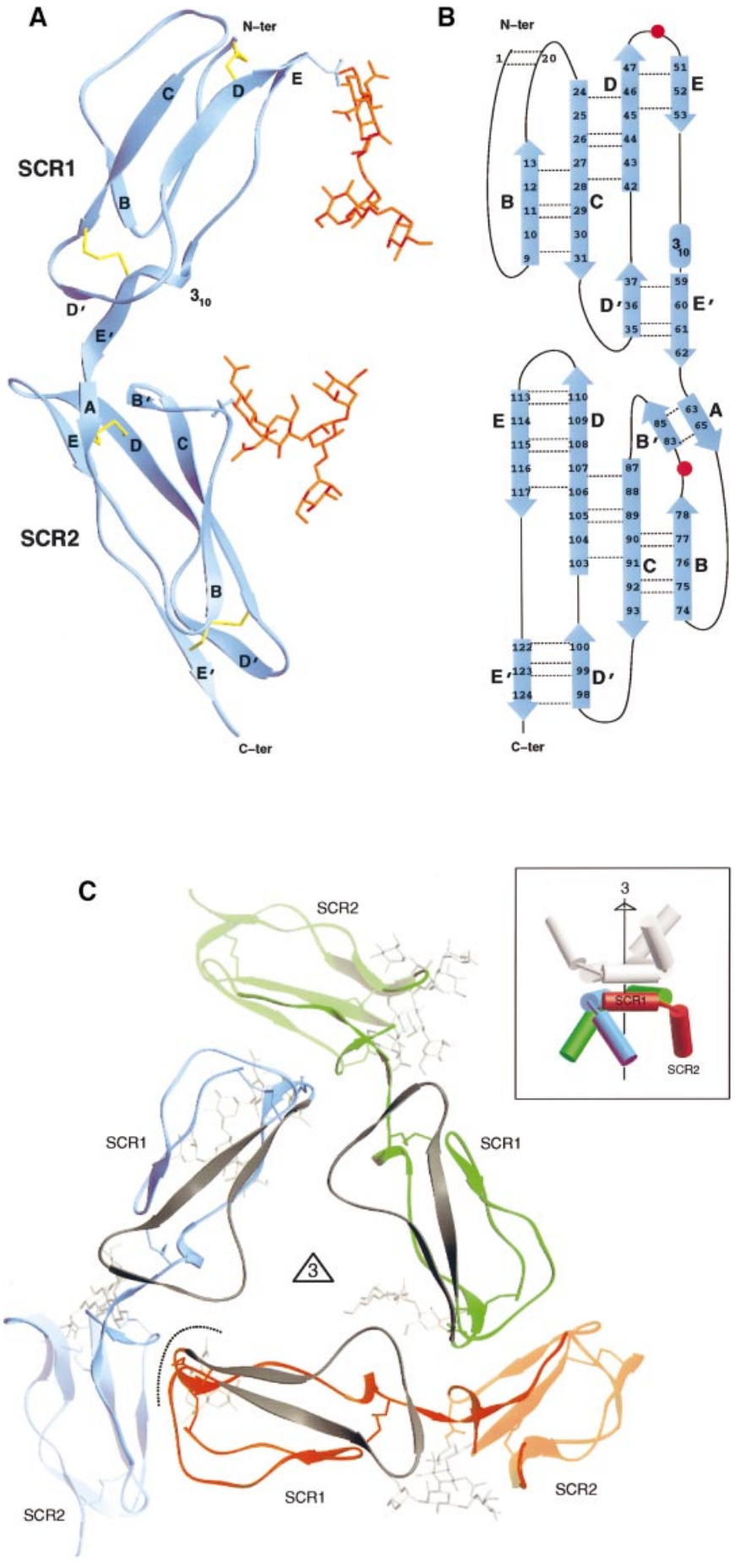
A
N–ter
SCR1
SCR2
C–ter
B
N–ter
C–ter
C
SCR2
SCR1
SCR1
SCR1
SCR2
SCR2
3

the available NMR structures of fragments of factor H (Barlow *et al*., 1993) and the vaccinia virus complement control protein (Wiles *et al*., 1997). Most of the available SCR structures contain a hydrogen bond between a main-chain carbonyl in the N-terminal coil segment and the side chain of the highly conserved tryptophan in strand E (not shown). This hydrogen bond and interactions between hydrophobic residues and the conserved prolines at the N-terminal coil of the domain link the coil to the central β-sheet. An additional hydrophobic contact that is present in most of the structures involves a proline between β-strands E and E′ and the conserved Tyr/Phe side chain in strand C (Figure 4A). On account of the similarity seen in the known structures, we expect the structure of the central β-sheet to be conserved in other SCR domains, and in particular in those of other RCA family members.

Despite a substantial degree of structural conservation for individual SCR domains, the three known structures of two-domain fragments differ strikingly in their inter-domain orientation (Figure 4B). The bend of ~60° between the two CD46 domains is similar to what is observed in the two-domain NMR structures (Barlow *et al*., 1993; Wiles *et al*., 1997). However, the N-terminal domain bends towards the DE-loop in the two NMR structures but away from this loop in CD46. Although it is possible that the interdomain orientation of the CD46 fragment is a result of intermolecular contacts in the crystal structure, we believe that the observed differences among the three structures are related mainly to differences in the DE-loop in the C-terminal repeat. An insertion between strands D and E in the second repeat of CD46 (Figure 4A) results in a highly protruding DE-loop, which sterically interferes with residues in the N-terminal domains of both NMR structures in the superimposed models (Figure 4B). The extended conformation of the DE-loop in CD46 SCR2 therefore favors an orientation in which the N-terminal domain of CD46 bends toward the opposite direction (Figure 4B).

We note that SCR domains can be grouped into two classes according to the presence or absence of an insertion of three or more residues between strands D and E (not shown), and we predict that in domains with such an insertion, the overall conformation of the corresponding two-domain fragment will be similar to that of CD46 SCR1–SCR2. This insertion is absent in SCR3 and SCR4 of CD46 and so it is possible for the conformations of the SCR2–SCR3 and SCR3–SCR4 segments to resemble those observed in the two NMR structures. However, since the relative orientations of the β-barrels also vary dramatically in all three structures (Figure 4B), information about the direction of the bend in a two-domain fragment alone is not sufficient to predict accurately the conformation of the entire four-domain CD46 molecule.

CD46 binding to measles virus

The two N-terminal repeats of CD46 are necessary and sufficient for binding of the receptor to the measles virus hemagglutinin (Iwata *et al*., 1995; Manchester *et al*., 1995; Nussbaum *et al*., 1995). In good correlation, anti-CD46 monoclonal antibodies that efficiently block binding to the measles virus hemagglutinin have been mapped to specific epitopes in SCR1 and SCR2 (Buchholz *et al*., 1997; Hsu *et al*., 1997). The critical binding epitopes for most of these anti-CD46 antibodies have been characterized through site-directed mutagenesis experiments (Figure 5A). Our crystal structure shows that the most inhibitory antibodies recognize surface residues located in the BC-loop, strand C and the DE-loop of SCR1, as well as a residue in the initial coil segment of SCR2 (Figure 4A). These residues are all located on the same face of the molecule (Figure 5A).

Additional information on virus interaction comes from binding studies with CD46-derived peptides (Manchester *et al*., 1997) and CD46 mutants (Buchholz *et al*., 1997; Hsu *et al*., 1997). The peptide-binding studies revealed two virus-binding epitopes, one located in SCR1 and the other in SCR2. The sequence Ile45–Cys46–Asp47–Arg48 at the end of strand D in SCR1 (Figure 4A) is common to several inhibitory peptides and is likely to contact the virus directly (orange in Figure 5B). Site-directed mutagenesis experiments have identified several additional residues in the vicinity of this sequence that are important for hemagglutinin binding. The location of these residues overlaps with antibody epitopes on SCR1 (Figure 5A and B), creating a virus-binding surface that is defined primarily by strands C and D.

Even though a long SCR2-derived peptide that extends from Phe85 to Ile104 was found to be inhibitory (Figure 4A), only residues 94–97 within the CD′-loop are close to the inhibitory antibody epitope on SCR2 and to Asp70 (Figure 5B), a residue with moderate contribution to binding of CD46 to both measles virus and soluble hemagglutinin (Buchholz *et al*., 1997). In addition, substitution of CD46 residues 94–105 with the homologous residues of CD55 abolished binding to hemagglutinin and did not support fusion of measles virus to the host cell (Mumenthaler *et al*., 1997). Taken together, these experiments strongly suggest that residues 94–97 have direct contacts with the virus and define another important virus-binding epitope at the base of SCR2, close to the beginning of strand B (Figure 5B). The virus-binding epitopes of SCR1 and SCR2 are located on the same side of the molecule (Figure 5A and B), which is free of carbohydrates and, therefore, easily accessible for protein–protein interactions.

The *N*-linked glycan attached to Asn80 in SCR2 has been shown to be essential for virus binding (Maisner

Fig. 2. Structure of the N-terminal two short consensus repeats SCR1 and SCR2 of CD46, and arrangement of the molecules in the crystal. (**A**) Ribbon drawing of the molecule. Disulfide bonds and carbohydrate residues are shown in yellow and red, respectively. (**B**) β-Sheet topology and secondary structure assignment. Main chain hydrogen bonds are indicated with dashed lines. Residues in β-strands were assigned based on main-chain hydrogen bond formation with a donor–acceptor distance of $\leqslant$3.5 Å. The glycosylation sites at Asn49 and Asn80 are marked with red spheres. (**C**) Arrangement of the six independent copies of the molecule in the crystal. Ribbon drawing of a trimer and schematic representation (inset) of two trimers present in the asymmetric unit of the crystals. The segments between strands C and D in the three SCR1 domains are located at the 'top' of the trimer and are colored in black. Each contact between two molecules buries a relatively large surface area of 1190 Å^2 and involves numerous hydrophobic residues (Ile22, Ile37, Pro38, Pro39, Leu40, Ile45 and Leu53). One such contact is marked with a broken line (lower left).

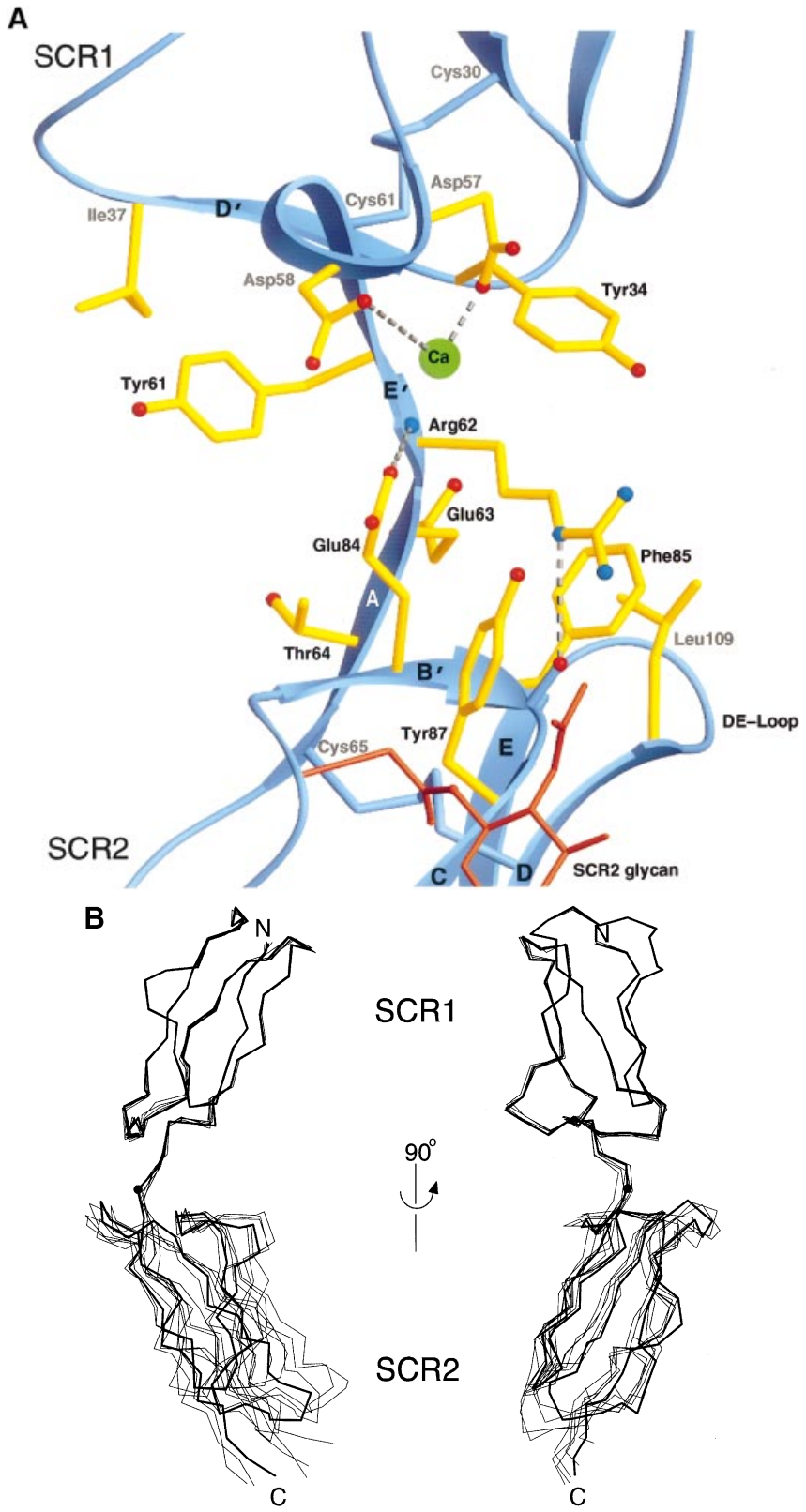

Fig. 3. Interdomain interface and movement between domains. (**A**) Detailed view of the interdomain interface. The main chain of a monomer is shown as a ribbon drawing with residues at the interface colored orange and Asn80 with the attached glycan colored red. Disulfide bonds are shown in blue, and hydrogen bonds are represented with broken lines. The calcium ion located at the interface is shown in green. Oxygen and nitrogen atoms are red and blue, respectively. Arg62 is hydrogen bonded to Glu84 and Phe85 in SCR2, and it is also within 4 Å of the aromatic ring of Tyr34 in SCR1. The remaining interactions at the interface involve hydrophobic contacts between (i) Tyr61 and Ile37, (ii) Phe85 and Leu109, and (iii) the methyl group of the first *N*-acetyl glucosamine of SCR2 and Tyr87. (**B**) Superposition of the six crystallographically independent molecules, showing the interdomain movement and the flexibility of the molecule at the domain interface. Two orthogonal views are given. The view on the left hand side is approximately parallel to the plane of maximum variation, and the view on the right hand side is approximately perpendicular to it. The superposition is based on residues within SCR1. The black sphere in the molecule drawn with thicker lines marks the kink in the polypeptide chain at Glu63, which is primarily responsible for the interdomain bend.

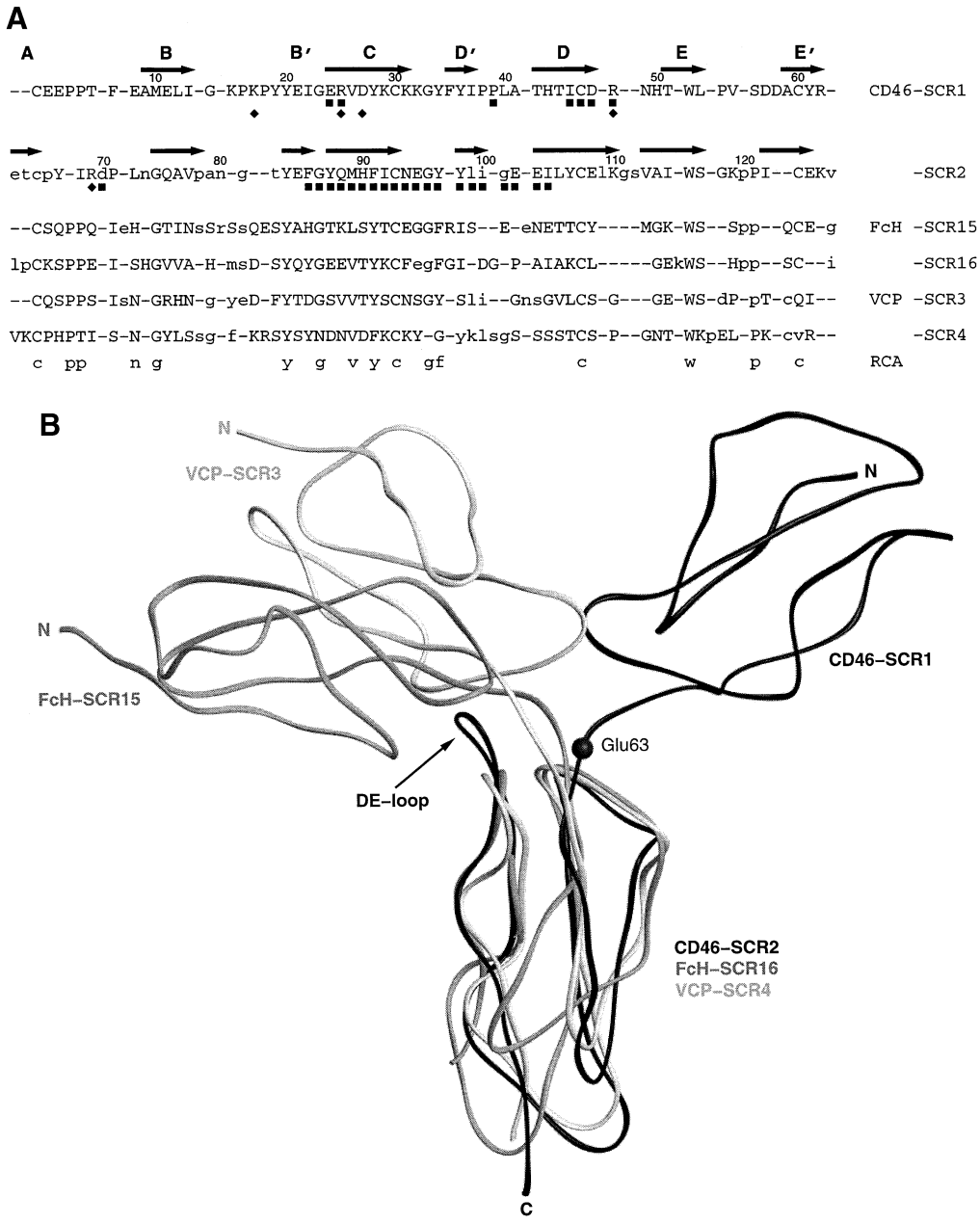

Fig. 4. Structural and orientational differences in fragments with two consecutive SCR domains. (**A**) Structural alignment of known SCR domains. CD46 SCR2, factor H (FcH) SCR15 and SCR16 (Barlow *et al.*, 1993) and vaccinia virus complement control protein (VCP) repeats SCR3 and SCR4 (Wiles *et al.*, 1997) were structurally aligned with CD46 SCR1 using MALIGN (Modeller; A.Sali, Rockefeller University, NY) with a gap penalty of 1.75. Residues whose C_α atoms are closer than 3.5 Å are shown in upper case, the remaining residues are in lower case. Residues that are conserved in most SCRs within the RCA family (based on sequence alignments of domains from CD46, CD55, CD35, CD21 and FcH) are also shown (RCA). CD46 residues involved in virus binding (■) or binding to antibodies that compete with measles virus hemagglutinin association (◆) are marked, and β-strands are represented with arrows. (**B**) Superimposed structures of CD46 SCR1–SCR2 (black), FcH SCR15–SCR16 [dark gray (Barlow *et al.*, 1993)] and VCP SCR3–SCR4 [light gray (Wiles *et al.*, 1997)]. The superposition is based on residues within the central β-sheet of the C-terminal repeats. The position of Glu63 in CD46 is marked with a sphere.

et al., 1996). It is located on the side opposite to the virus-binding surface (Figure 5A and B) and makes hydrophobic contacts with residues Tyr87 and Ile104 in all six crystallographically independent copies of the molecule. Therefore, we do not expect this carbohydrate to contact the virus, but we believe that it stabilizes the conformation of the virus-binding surface through interactions with protein residues.

The virus recognition surface in SCR1 is located at the top of the trimers found in the crystal (black in Figure 2C), and it is therefore available for interactions in such an arrangement of the molecule. The virus-binding epitopes at the base of SCR2 are also exposed and easily accessible from the top of the trimer. The CD46 trimer would therefore be well suited for interaction with a trimeric ligand. Even though receptor-binding proteins in the envelopes of alphaviruses, retroviruses and influenza virus form trimeric clusters (Garoff *et al.*, 1998), it is unclear how the envelope proteins of measles virus are organized, and whether the hemagglutinin protein forms

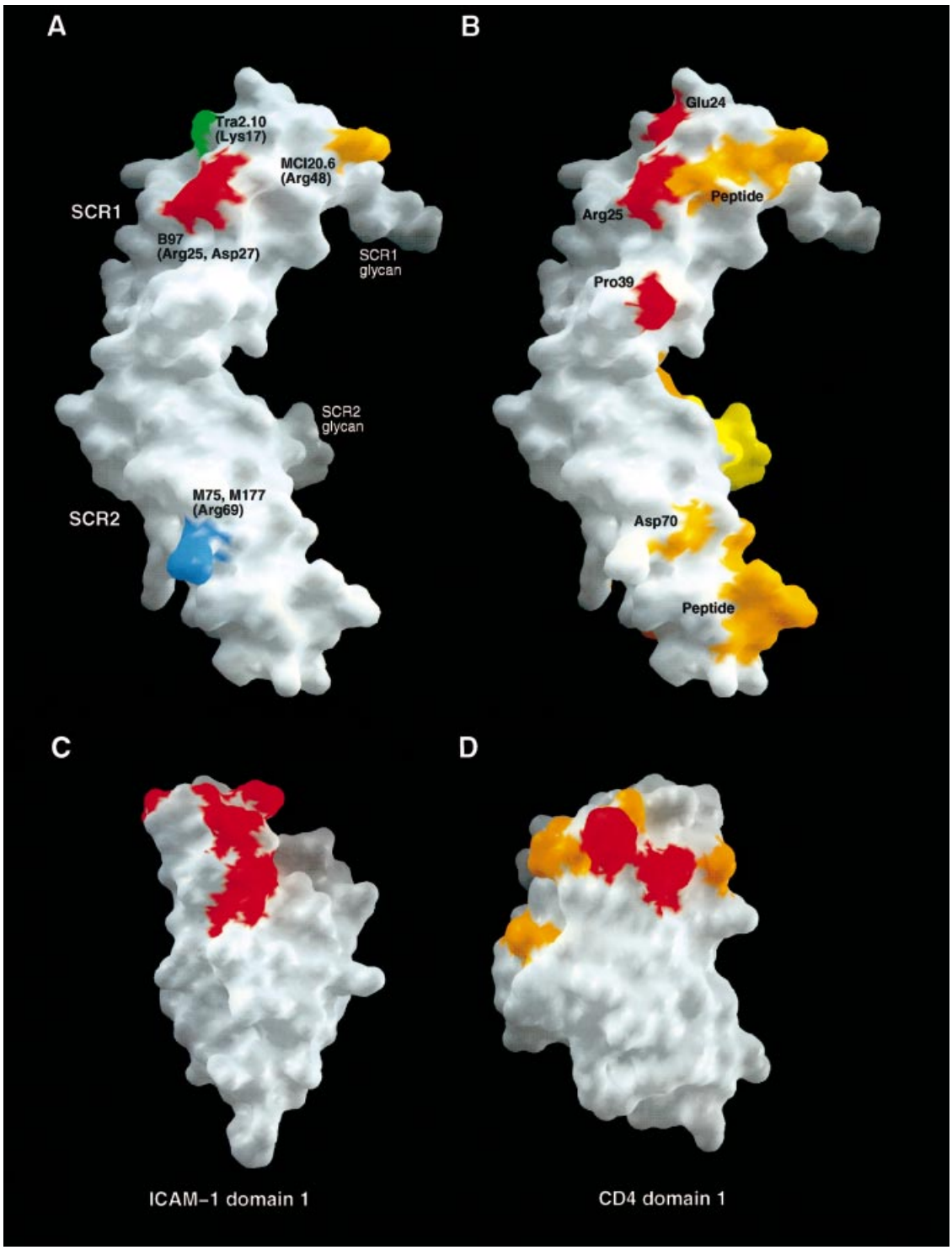

Fig. 5. Virus-binding surfaces in human virus receptors CD46, ICAM-1 and CD4. (A and B) Surface representations of the N-terminal two repeats of CD46 with epitopes for antibody and measles virus binding. (**A**) Epitopes for anti-CD46 monoclonal antibodies that significantly blocked virus binding to the receptor (inhibitory effect >50% in Buchholz *et al*., 1997; Hsu *et al*., 1997). Residues recognized by B97, Tra2.10, MCI20.6, M75 and M177 antibodies are colored. (**B**) Regions involved in measles virus binding. Residues Glu24, Arg25 and Pro39 had a severe effect on hemagglutinin binding according to mutagenesis experiments (Buchholz *et al*., 1997; Hsu *et al*., 1997) and are shown in red. Residue Asp70 had a moderate effect on binding of CD46 to both measles virus and soluble hemagglutinin and is marked in orange. Stretches of amino acids 45–48 and 85–104 that were identified by peptide inhibition studies (Manchester *et al*., 1997) are shown in orange. The carbohydrate bound to SCR2 is shown in yellow. The view of the molecule is similar to that in Figure 2A. (**C**) Surface representation of the N-terminal domain of ICAM-1 (Casasnovas *et al*., 1998). Residues Gln27, Pro28, Lys29, Leu30, Tyr66, Pro70 and Asp71 that are involved in interaction with several human rhinoviruses are shown in red. (**D**) Surface representation of the N-terminal domain of CD4 (Kwong *et al*., 1998). Phe43 and Arg59, the two residues that interact primarily with human immunodeficiency virus (HIV) (Kwong *et al*., 1998), are shown in red; residues Gln25, Lys29, Lys35, Gln40, Ser42 and Ser60 make additional contacts and are shown in orange. The coordinates for ICAM-1 (Casasnovas *et al*., 1998) and the CD4–gp120 complex (Kwong *et al*., 1998) were obtained from the Brookhaven Protein Data Bank (accession codes 1IC1 and 1GC1). Only the side chains of residues are colored in (A–D).

trimers that are suitable for interaction with a trimeric receptor.

Virus-binding surfaces and virus–receptor interactions

Prior to this work, virus recognition sites have been defined in the three-dimensional structures of three human cell surface receptors: (i) CD4, the HIV receptor (Wang *et al*., 1990; Ryu *et al*., 1990; Kwong *et al*., 1998); (ii) ICAM-1, the rhinovirus receptor (Bella *et al*., 1998; Casasnovas *et al*., 1998); and (iii) the I domain of the α2β1 integrin, a receptor for echovirus 1 (King *et al*., 1997). In all three cases, virus recognition involves a single domain. Structural information about the virus–receptor complex is available only for CD4 and ICAM-1 (Bella *et al*., 1998; Kwong *et al*., 1998). Both of these molecules belong to the immunoglobulin superfamily, and in both cases virus recognition is limited to a small area that lies within the N-terminal domain, distal to the membrane surface (Figure 5C and D). This mode of interaction is conceptually very different from the one utilized by virus receptors that belong to the RCA family. The three known virus receptors in this family (CD21, CD55 and CD46) all use two or more consecutive domains for virus recognition (Molina *et al*., 1991; Clarkson *et al*., 1995; Iwata *et al*., 1995; Manchester *et al*., 1995). Therefore, interdomain orientation and movement between domains are parameters that will critically affect virus binding in all three cases. The crystal structure presented here reveals some flexibility between the two CD46 repeats (Figure 3B), and this flexibility may facilitate binding of the first and second repeats of the receptor to the measles virus hemagglutinin.

A recent analysis of electron microscopy data obtained from a complex between ICAM-1 and rhinovirus has shown that the N-terminal domain of ICAM-1 fits into a recessed receptor-binding site or 'canyon' that is present on the viral capsid (Bella *et al*., 1998). A number of residues at the tip of the ICAM-1 domain (red in Figure 5C) contact the floor of this canyon, which has the most conserved residues among different rhinovirus serotypes (Rossmann, 1989). Although HIV is an enveloped virus that lacks such canyons, the recent crystal structure of the HIV envelope glycoprotein gp120 in complex with CD4 (Kwong *et al*., 1998) exhibits interesting parallels and similarities to the rhinovirus–ICAM-1 interaction. In particular, the HIV glycoprotein also recognizes the most membrane-distal region of the N-terminal CD4 domain, which is inserted into a recessed surface on gp120 (Figure 5D). At the center of the interaction between gp120 and CD4 lies the critical CD4 residue Phe43, which penetrates deeply into a gp120 cavity lined with hydrophobic residues that are conserved among different virus strains. CD4 residues surrounding Phe43 and other residues at the tip of the domain also contact gp120 (Figure 5D). Thus, the two recent studies on virus–receptor interactions show that both rhinoviruses and HIV use recessed binding sites for receptor recognition. Such a mode of binding is likely to be part of an efficient mechanism through which viruses hide their receptor-binding epitopes from immune surveillance (Rossmann, 1989).

The virus-binding residues of ICAM-1 and CD4 cluster within a small area at the tip of the N-terminal domain, with maximum distances between residues of ~20 Å for ICAM-1 and ~30 Å for CD4. By contrast, the virus-binding residues in CD46 are quite distant from each other, defining a surface that extends over two complete SCRs and spanning a distance of ~60 Å (Figure 5A and B). The large differences in shape and size between the binding surface in CD46 and the surfaces in CD4 and ICAM-1 strongly suggest that the CD46 virus recognition mode differs from that seen in the two members of the immunoglobulin superfamily. It is very unlikely that the extended binding surface in CD46 can fit into a single narrow and recessed binding site, and we therefore predict that the measles virus hemagglutinin protein itself has an extended receptor-binding surface, possibly with several binding sites. These sites, and perhaps also the receptor-binding regions of related paramyxoviruses, must be less recessed and more accessible than the binding surfaces in HIV and rhinoviruses.

The D′D-loop of CD46 SCR1, a critical virus-binding site

The CD46 virus-binding surface is corrugated, containing several ridges and crevices that could be important for proper attachment of the viral hemagglutinin. A particularly prominent ridge at the center of the virus-binding surface is created by a protruding loop between strands D′ and D in SCR1 (see Figure 2A) that is located at the domain interface and contains the critical virus-binding residue Pro39 (Figure 5B). Extensive mutagenesis experiments on CD46 showed that the mutation Pro39 to Ala39 had a large effect on binding to the measles virus hemagglutinin (Buchholz *et al*., 1997). This suggests that the D′D-loop is indeed a critical binding site.

As shown in Figure 6, the D′D-loop of SCR1 has a rather open, semi-circular conformation that is stabilized in part by interactions between Tyr36 and several residues within the loop. The D′D-loop is highly unusual in that all of its residues (Ile37, Pro38, Pro39, Leu40 and Ala41) are completely hydrophobic and largely accessible to solvent. This non-polar loop structure at the center of the virus–receptor binding interface might well fit into a hydrophobic crevice on the viral hemagglutinin, and we therefore expect several residues within the D′D-loop to participate in virus binding. The critical role of Pro39, which projects furthest from the domain, might resemble that of Phe43 in the CD4–gp120 interaction. The polar residues in the vicinity of the D′D-loop in SCR1 may provide a more modest contribution to this interaction, as suggested by mutants in this region (Figure 5B). Some residues at the bottom of SCR2 are likely to also have an important role in binding of CD46 to the hemagglutinin protein, but further characterization of this binding site is needed to establish the precise function of these residues.

Conclusions

The structure presented here extends our knowledge of SCR domain function in complement regulation and virus recognition. The use of several flexibly linked domains with expansive epitopes for interactions with viruses or complement is likely to be conserved in other members of the RCA family. Many of these proteins use more than a single SCR domain for protein–protein interactions, and the available structures of two-domain SCR fragments of

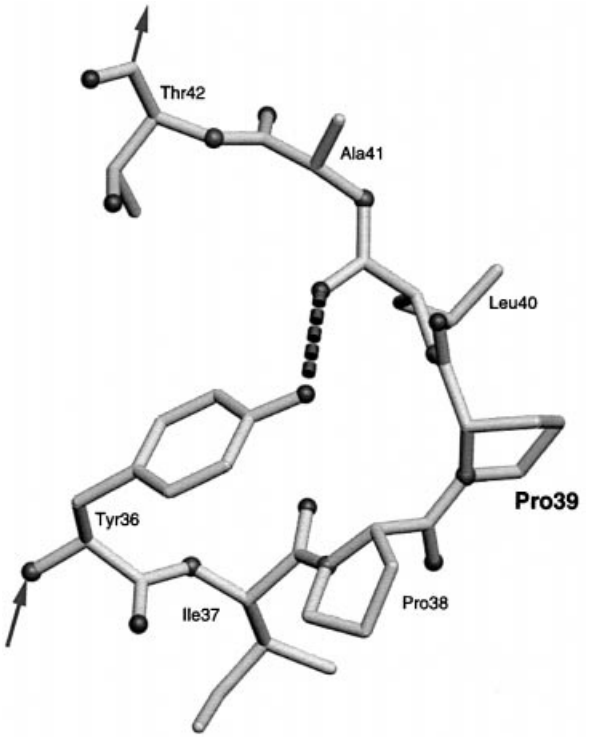

Fig. 6. Atomic structure of the highly hydrophobic D′D-loop of SCR1. The critical proline at position 39 is labeled in bold. The hydrogen bond between the hydroxyl group of Tyr36 and the main-chain carbonyl of Leu40 is shown with a broken line. This hydrogen bond is present in all six independent copies of the molecule. In addition to Leu40, the Tyr36 side chain is also within 4 Å of Ile37, Pro38 and Pro39. Note that Pro39 is in a *cis* conformation.

CD46, factor H (Barlow *et al*., 1993) and the vaccinia virus complement control protein (Wiles *et al*., 1997) all indicate that some degree of interdomain flexibility is an inherent property of molecules constructed from concatenated SCR domains. We show that although the main architecture of SCR domains is conserved in all three structures, the molecules differ dramatically in their interdomain orientation. As is the case for CD46, interactions involving many other SCR-containing proteins will depend critically on the orientation between consecutive domains and may require some interdomain flexibility.

The extended virus-binding surface seen in the crystal structure of CD46 suggests that the receptor-contacting area of measles virus must be larger and more exposed than the ligand-binding sites described for HIV and rhinoviruses. Nevertheless, we propose that the CD46–measles virus hemagglutinin and CD4–HIV gp120 interactions have a similar critical hydrophobic contact at the center of their binding interfaces. If this is indeed the case, molecules or cyclic peptides that mimic the protruding D′D-loop in SCR1 of CD46 could be very effective anti-viral agents. Despite the availability of an effective attenuated live vaccine, measles outbreaks continue to occur in industrialized nations and are a leading cause of morbidity and mortality in children worldwide (Griffin and Bellini, 1996). The significant failure rate with current vaccines (Edmonson *et al*., 1996) prompts the development of new therapies. The CD46 structure provides new information for the design of virus inhibitors which, combined with further characterization of the interaction between measles virus and CD46, will lead to new strategies to treat and prevent measles virus infections.

Materials and methods

Protein production

A recombinant cDNA fragment with the region coding for residues Met1–Val160 of the precursor CD46 protein followed by a translation stop codon was generated by PCR using *Pfu*I polymerase (Stratagene) and subcloned into the expression vector pBJ5-GS. The recombinant protein was expressed in CHO Lec. 3.2.8.1 cells (Stanley, 1989) using the glutamine synthetase system (Casasnovas *et al*., 1998). Recombinant protein was purified from cell culture supernatant of selected cell clones using affinity chromatography with concanavalin A–Sepharose and size exclusion chromatography with Superdex-200 (Pharmacia Biotech). N-terminal sequencing revealed that the first residue of the mature recombinant protein was Cys35 of the precursor protein.

Structure determination and analysis

Crystals were grown at 20°C using the hanging drop method by mixing equal volumes of reservoir buffer (16% PEG 8K, 40 mM $CaCl_2$, 100 mM Na cacodylate pH 6.5) and 7 mg/ml protein. The crystals belong to space group $P2_12_12_1$ (a = 74.5 Å, b = 111.1 Å and c = 137.5 Å) and contain six molecules in their asymmetric unit. Crystals were soaked for 30 min in reservoir buffer supplemented with 25% ethylene glycol before flash-freezing them in liquid nitrogen. Diffraction data were collected at 100 K with an RAXIS IV detector (Molecular Structure Corp.) and Cu K_α radiation. A native data set that extends to 3.1 Å resolution and consists of 19 637 unique reflections was recorded at beamline X12B of the National Synchrotron Light Source (Brookhaven National Laboratory) using an ADS Quantum 4 CCD detector. Data were integrated and reduced using the HKL package (Otwinowski and Minor, 1997). Derivatives were prepared by soaking crystals in solutions containing heavy atom compounds at various concentrations (Table I), and heavy atom-binding sites were determined using difference Patterson and difference Fourier techniques. Difference Patterson maps were calculated with normalized structure factors and interpreted manually. Heavy atom sites were refined and phases were calculated with MLPHARE (CCP4, 1994). The final figure of merit was 0.55 (25–3.4 Å). Data collection and phasing statistics are given in Table I.

Solvent flattening and histogram matching with DM (CCP4, 1994) significantly improved the initial electron density map, allowing us to assign domain boundaries and calculate non-crystallographic symmetry (NCS) operators. For averaging and refinement, native data were sharpened with a B-factor of –40 $Å^2$. Refinement of symmetry operators and domain-wise averaging were carried out with RAVE (Kleywegt and Jones, 1994). SCR1 could be traced easily in the 6-fold averaged map. Since several loops in SCR2 vary in structure, they were poorly visible in the averaged maps and were built using the original solvent-flattened map. The model was built with O (Jones *et al*., 1991) and refined at 3.1 Å with X-PLOR (Brünger *et al*., 1987) using bulk solvent correction, anisotropic temperature factor scaling and NCS restraints. The final model contains all protein atoms (6× residues 1–126), six calcium ions, 12 well-ordered water molecules and 12 *N*-linked glycans of varying length. The N-terminal domain, SCR1, is very well ordered and has similar average temperature factors (ranging from 60 to 68 $Å^2$) in all six copies; in contrast, the six average temperature factors for the second domain, SCR2, range from 66 to 130 $Å^2$. Several residues in the two SCR2 domains with the highest temperature factors are not well defined. Surface areas were calculated with SURFACE (CCP4, 1994) using a probe radius of 1.4 Å. The quoted numbers represent the total areas buried in both interacting partners. Coordinates for two-domain fragments of factor H (Barlow *et al*., 1993) and vaccinia virus complement control protein (Wiles *et al*., 1997) were obtained from the Brookhaven Protein Data Bank (accession codes 1HFH and 1VVC). Figure 1 was prepared with BOBSCRIPT (Esnouf, 1997), Figures 2, 3A, 4B and 6 with RIBBONS (Carson, 1987), Figure 3B with MOLSCRIPT (Kraulis, 1991) and Figure 5 with GRASP (Nicholls *et al*., 1991).

Acknowledgements

We acknowledge Brookhaven National Laboratory for access to beamline X12B, and we thank Malcolm Capel and the Brookhaven staff for their competent assistance. We also thank Steve Harrison and Alan Ezekowitz for comments on the manuscript, and Roberto Cattaneo for recombinant

CD46 cDNA. J.M.C. acknowledges support from KI-NOVUM and thanks Holland Cheng for making his computer graphics system available. M.L. is a predoctoral fellow of the Howard Hughes Medical Institute. Supported by departmental funds from Massachusetts General Hospital (T.S.). Coordinates have been deposited with the Brookhaven Protein Data Bank (accession code 1CKL) and are also available from the authors.

References

Adams,E.M., Brown,M.C., Nunge,M., Krych,M. and Atkinson,J.P. (1991) Contribution of the repeating domains of membrane cofactor protein (CD46) of the complement system to ligand binding and cofactor activity. *J. Immunol.*, **147**, 3005–3011.

Barlow,P.N., Steinkasserer,A., Norman,D.G., Kieffer,B., Wiles,A.P., Sim,R.B. and Campbell,I.D. (1993) Solution structure of a pair of complement modules by nuclear magnetic resonance. *J. Mol. Biol.*, **232**, 268–284.

Bella,J., Kolatkar,P.R., Marlor,C.W., Greve,J.M. and Rossmann,M.G. (1998) The structure of the two amino-terminal domains of human ICAM-1 suggests how it functions as a rhinovirus receptor and as an LFA-1 integrin ligand. *Proc. Natl Acad. Sci. USA*, **95**, 4140–4145.

Bergelson,J.M., Chan,M., Solomon,K.R., St. John,N.F., Lin,H. and Finberg,R.W. (1994) Decay-accelerating factor (CD55), a glycosylphosphatidyl-inositol-anchored complement regulatory protein, is a receptor for several echoviruses. *Proc. Natl Acad. Sci. USA*, **91**, 6245–6249.

Bergelson,J.M., Modlin,J.F., Wieland-Alter,W., Cunningham,J.A., Crowell,R.L. and Finberg,R.W. (1997) Clinical coxsackievirus B isolates differ from laboratory strains in their interaction with two cell surface receptors. *J. Infect. Dis.*, **175**, 697–700.

Bork,A., Downing,A.K., Kieffer,B. and Campbell,I.D. (1996) Structure and distribution of modules in extracellular proteins. *Q. Rev. Biophys.*, **29**, 119–167.

Brünger,A.T. (1992) Free *R* value: a novel statistical quantity for assessing the accuracy of crystal structures. *Nature*, **355**, 472–475.

Brünger,A.T., Kuriyan,J. and Karplus,M. (1987) Crystallographic *R*-factor refinement by molecular dynamics. *Science*, **235**, 458–460.

Buchholz,C.J., Koller,D., Devaux,P., Mumenthaler,C., Schneider-Schaulies,J., Braun,W., Gerlier,D. and Cattaneo,R. (1997) Mapping of the primary binding sites of measles virus to its receptor CD46. *J. Biol. Chem.*, **272**, 22072–22079.

Carson,M. (1987) Ribbon models of macromolecules. *J. Mol. Graph.*, **5**, 103–106.

Casasnovas,J.M., Stehle,T., Liu,J.H., Wang,J.H. and Springer,T.A. (1998) A dimeric crystal structure for the N-terminal two domains of intercellular adhesion molecule-1. *Proc. Natl Acad. Sci. USA*, **95**, 4134–4139.

CCP4 (1994) The CCP4 suite: programs for protein crystallography. *Acta Crystallogr.*, **D50**, 760–763.

Christiansen,D., Milland,J., Thorley,B.R., McKenzie,I.F.C., Mottram,P.L., Purcell,L.J. and Loveland,B.E. (1996) Engineering of recombinant soluble CD46: an inhibitor of complement activation. *Immunology*, **87**, 348–354.

Clarkson,N.A., Kaufman,R., Lublin,D.M., Ward,T., Pipkin,P.A., Minor,P.D., Evans,D.J. and Almond,J.W. (1995) Characterization of the echovirus 7 receptor: domains of CD55 critical for virus binding. *J. Virol.*, **69**, 5497–5501.

Dörig,R.E., Marcil,A., Chopra,A. and Richardson,C.D. (1993) The human CD46 molecule is a receptor for measles virus. *Cell*, **75**, 295–305.

Edmonson,M.B., Davis,J.P., Hopfensperger,D.J., Berg,J.L. and Payton,L.A. (1996) Measles vaccination during the respiratory virus season and risk of vaccine failure. *Pediatrics*, **98**, 905–910.

Esnouf,R.M. (1997) An extensively modified version of MolScript that includes greatly enhanced colouring capabilities. *J. Mol. Graph. Model.*, **15**, 132–134.

Fingeroth,J.D., Weis,J.J., Tedder,T.F., Strominger,J.L., Biro,P.A. and Fearon,D.T. (1984) Epstein–Barr virus receptor of human B lymphocytes is the C3d receptor CR2. *Proc. Natl Acad. Sci. USA*, **81**, 4510–4514.

Garoff,H., Hewson,R. and Opstelten,D.J. (1998) Virus maturation by budding. *Microbiol. Mol. Biol. Rev.*, **62**, 1171–1190.

Griffin,D.E. and Bellini,W.J. (1996) Measles virus. In Fields,B.N., Knipe,D.M. and Howley,P.M. (eds), *Fields Virology.* 3rd edn. Lippincott-Raven, Philadelphia/New York, pp. 1267–1312.

Hara,T., Kuriyama,S., Kiyohara,H., Nagase,Y., Matsumoto,M. and Seya,T. (1992) Soluble forms of membrane cofactor protein (MCP, CD46) are present in plasma, tears and seminal fluid in normal subjects. *Clin. Exp. Immunol.*, **89**, 490–494.

Hsu,E.C., Dörig,R.E., Sarangi,F., Marcil,A., Iorio,C. and Richardson,C.D. (1997) Artificial mutations and natural variations in the CD46 molecules from human and monkey cells define regions important for measles virus binding. *J. Virol.*, **71**, 6144–6154.

Hsu,E.C. *et al*. (1998) A single amino acid change in the hemagglutinin protein of measles virus determines its ability to bind CD46 and reveals another receptor on marmoset B cells. *J. Virol.*, **72**, 2905–2916.

Iwata,K., Seya,T., Yanagi,Y., Pesando,J.M., Johnson,P.M., Okabe,M., Ueda,S., Ariga,H. and Nagasawa,S. (1995) Diversity of sites for measles virus binding and for inactivation of complement C3b and C4b on membrane cofactor protein CD46. *J. Biol. Chem.*, **270**, 15148–15152.

Jones,T.A., Zhou,J.Y., Cowan,S.W. and Kjeldgaard,M. (1991) Improved methods for building protein models in electron density maps and the location of errors in these models. *Acta Crystallogr.*, **A47**, 110–119.

Karp,C.L., Wysocka,M., Wahl.,L.M., Ahearn,J.M., Cuomo,P.J., Sherry, B., Trinchieri,G. and Griffin,D.E. (1996) Mechanism of suppression of cell-mediated immunity by measles virus. *Science*, **273**, 228–231.

King,S.L., Kamata,T., Cunningham,J.A., Emsley,J., Liddington,R.C., Takada,Y. and Bergelson,J.M. (1997) Echovirus 1 interaction with the human very late antigen-2 (integrin $\alpha 2\beta 1$) I domain. *J. Biol. Chem.*, **272**, 28518–28522.

Kleywegt,G.J. and Jones,T.A. (1994) Halloween...masks and bones. In Bailey,S., Hubbard,R. and Waller,D. (eds), *From First Map to Final Model.* SERC Daresbury Laboratory, Warrington, UK, pp. 59–66.

Kraulis,P.J. (1991) MOLSCRIPT: a program to produce both detailed and schematic plots of protein structures. *J. Appl. Crystallogr.*, **24**, 946–950.

Kwong,P.D., Wyatt,R., Robinson,J., Sweet,R.W., Sodroski,J. and Hendrickson,W.A. (1998) Structure of an HIV gp120 envelope glycoprotein in complex with the CD4 receptor and a neutralizing antibody. *Nature*, **393**, 648–659.

Liszewski,M.K., Post,T.W. and Atkinson,J.P. (1991) Membrane cofactor protein (MCP or CD46): newest member of the regulators of complement activation gene cluster. *Annu. Rev. Immunol.*, **9**, 431–455.

Lublin,D.M., Liszewski,M.K., Post,T.W., Arce,M.A., LeBeau,M.M., Rebentisch,M.B., Lemons,R.S., Seya,T. and Atkinson,J.P. (1988) Molecular cloning and chromosomal localization of human membrane cofactor protein (MCP) *J. Exp. Med.*, **168**, 181–194.

Maisner,A., Alvarez,J., Liszewski,M.K., Atkinson,D.J., Atkinson,J.P. and Herrler,G. (1996) The *N*-glycan of the SCR2 region is essential for membrane cofactor protein (CD46) to function as a measles virus receptor. *J. Virol.*, **70**, 4973–4977.

Manchester,M., Valsamakis,A., Kaufman,R., Liszewski,M.K., Alvarez,J., Atkinson,J.P., Lublin,D.M. and Oldstone,M.B.A. (1995) Measles virus and C3 binding sites are distinct on membrane cofactor protein. *Proc. Natl Acad. Sci. USA*, **92**, 2303–2307.

Manchester,M., Gairin,J.E., Patterson,J.B., Alvarez,J., Liszewski,M.K., Eto,D.S., Atkinson,J.P. and Oldstone,M.B.A. (1997) Measles virus recognizes its receptor, CD46, via two distinct binding domains within SCR1–2. *Virology*, **233**, 174–184.

McLaughlin,P.J., Holland,S.J., Taylor,C.T., Olah,K.S., Lewis-Jones,D.I., Hara,T., Seya,T. and Johnson,P.M. (1996) Soluble CD46 (membrane cofactor protein, MCP) in human reproductive fluids. *J. Reprod. Immunol.*, **31**, 209–219.

Molina,H., Brenner,C., Jacobi,S., Gorka,J., Carel,J.C., Kinoshita,T. and Holers,V.M. (1991) Analysis of Epstein–Barr virus binding sites on complement receptor 2 (CR2/CD21) using human–mouse chimeras and peptides. At least two distinct sites are necessary for ligand–receptor interaction. *J. Biol. Chem.*, **266**, 12173–12179.

Mumenthaler,C., Schneider,U., Buchholz,C.J., Koller,D., Braun,W. and Cattaneo,R. (1997) A 3D model for the measles virus receptor CD46 based on homology modeling. Monte Carlo simulations, and hemagglutination binding studies. *Protein Sci.*, **6**, 588–597.

Naniche,D., Varior-Krishnan,G., Cervoni,F., Wild,T.F., Rossi,B., Rabourdin-Combe,C. and Gerlier,D. (1993) Human membrane cofactor protein (CD46) acts as a cellular receptor for measles virus. *J. Virol.*, **67**, 6025–6032.

Nicholls,A., Sharp,K.A. and Honig,B. (1991) Protein folding and association: insights from the interfacial and the thermodynamic properties of hydrocarbons. *Proteins Struct. Funct. Genet.*, **11**, 281–296.

Nussbaum,O., Broder,C.C., Moss,B., Stern,L.B., Rozenblatt,S. and Berger,E.A. (1995) Functional and structural interactions between measles virus hemagglutinin and CD46. *J. Virol.*, **69**, 3341–3349.

Otwinowski,Z. and Minor,W. (1997) Processing of X-ray diffraction data collected in oscillation mode. *Methods Enzymol.*, **276**, 307–326.

Patterson,J.B., Scheiflinger,F., Manchester,M., Yilma,T. and Oldstone,M.B.A. (1999) Structural and functional studies of the measles virus hemagglutinin: identification of a novel site required for CD46 interaction. *Virology*, **256**, 142–151.

Rossmann,M.G. (1989) The canyon hypothesis. Hiding the host cell receptor attachment site on a viral surface from immune surveillance. *J. Biol. Chem.*, **264**, 14587–14590.

Ryu,S.E. *et al*. (1990) Crystal structure of an HIV-binding recombinant fragment of human CD4. *Nature*, **348**, 419–426.

Seya,T., Turner,J. and Atkinson,J.P. (1986) Purification and characterization of a membrane protein (gp45-70) that is a cofactor for cleavage of C3b and C4b. *J. Exp. Med.*, **163**, 837–855.

Stanley,P. (1989) Chinese hamster ovary cell mutants with multiple glycosylation defects for production of glycoproteins with minimal carbohydrate heterogeneity. *Mol. Cell. Biol.*, **9**, 377–383.

Wang,J.H. *et al*. (1990) Atomic structure of a fragment of human CD4 containing two immunoglobulin-like domains. *Nature*, **348**, 411–418.

Ward,T., Pipkin,P.A., Clarkson,N.A., Stone,D.M., Minor,P.D. and Almond,J.W. (1994) Decay-accelerating factor CD55 is identified as the receptor for echovirus-7 using CELICS, a rapid immuno-focal cloning method. *EMBO J.*, **13**, 5070–5074.

Wiles,A.P., Shaw,G., Bright,J., Perczel,A., Campbell,I.D. and Barlow,P.N. (1997) NMR studies of a viral protein that mimics the regulators of complement activation. *J. Mol. Biol.*, **272**, 253–265.

Received February 15, 1999; revised and accepted April 8, 1999